

# CUMULATIVE METHOD OF THE IMAGE RECONSTRUCTION IN SYNTHETIC APERTURE. EXPERIMENTAL RESULTS

JANUSZ WOJCIK, IHOR TROTS, MARCIN LEWANDOWSKI,  
ANDRZEJ NOWICKI

Institute of Fundamental Technological Research, Polish Academy of Sciences  
Pawińskiego 5b 02-106 Warsaw, Poland  
jwojcik@ippt.gov.pl

*An analytical model of imaging using synthetic aperture (SA) methods is presented. This model takes into account: fundamental features of an environment, of an electric transmission/reception path and a description of SA structure – possible schemes of transmission, reception and image formation. Then two schemes are analyzed: a proposed cumulative synthetic transmit aperture (CSTA) and for comparison of the standard STA schemes. For both methods identical basic parameters – equal sequences of transmit and receive transducers were applied. The distinctive feature of CSTA is gathering (summing up) echoes of subsequent transmissions in one acquisition matrix sufficient for image reconstruction. In traditionally applied STA methods a separate acquisition matrix for each transmission is created. Therefore there are a dozen to several dozen more matrices and the time of image reconstruction is at least several times longer than in CSTA. The presented experimental results obtained using wire and tissue mimicking phantoms have shown the comparable imaging quality in both methods.*

## INTRODUCTION

The SA method provides a new solution in ultrasound diagnostics and has particular importance in applications where frame rate and image resolution play a decisive role. In particular these are entirely new areas of application in cardiology e.g. to study the dynamics of the heart wall motion. The other very important application is the treatment of cancer using focused ultrasound [1]. It has to be noticed that high resolution imaging enables more accurate diagnostics of examined pathologic changes and consequently earlier and better therapy.

The application of synthetic aperture is a radical change compared to currently used scanners where the image is created line by line. So far in ultrasonography the way of image

formation considerably limits resolution, acquisition speed and the possibility of obtaining sufficient imaging data of high quality. The synthetic aperture method allows to solve these problems since on account of wide spatial spectrum of constituent elements it allows to obtain data in a wide angular range simultaneously during several transmissions and after that the whole ultrasound image is created [2].

Optimization in the SA method consists in finding the optimal relation between memory size, reconstruction time and computational power necessary for the acquisition of the echoes from an imaged object and reconstruction of its high-quality image.

The aim of the SA optimization (in weak “local” formulation) is to minimize the parameters mentioned before and to decrease the cost while maintaining the acceptable image quality – in comparison to known or applied methods.

The presented results concern examination and implementation of the ultrasound field in the SA method, which solve the above mentioned problem.

In section 1 the analytical model of imaging in SA methods is presented. The model takes into account: fundamental features of an environment, electric transmission/reception path, geometry of the transmission/reception system and description of SA structure – SA structural matrix including possible schemata of transmission and reception and of image reconstruction. While providing the transmission/reception description of the general SA model the solutions of Rayleigh-Sommerfeld to boundary-value problems of Dirichlet and Neumann are used. Then the two schemata isolated from the structural matrix are analyzed. The proposed cumulative synthetic transmit aperture (CSTA) and for comparison one of the standard synthetic transmit aperture (STA) schemata are described. The isolation of CSTA was made by a complex (therefore omitted here) spectral analysis of the general SA model.

In section 2 the two methods are described in detail. The diagram of echo transmission and reception and the principles of image reconstruction are presented. For both methods identical basic parameters – equal sequences of transmit and receive transducers were applied. The distinctive feature of CSTA is summing up echoes of subsequent transmissions in one sufficient for image synthesis acquisition matrix. In traditionally applied STAs a separate acquisition matrix for each transmission is created. Therefore there are a dozen to several dozen more matrices and the time of image synthesis is at least several times longer than in CSTA.

In section 3 the results of comparative experiments carried out using wire and tissue RMI phantoms and applying a programmable ultrasound scanner ULTRASONIX are presented. The results have shown the comparable imaging quality of both methods. But the ‘cost’ of obtaining the image is at least several times lower in the CSTA method.

## 1. PHYSICAL MODEL

The proposed physical model describing acoustic field generation, its propagation in a heterogeneous medium and detection is based on Sturm-Liouville equation (modified Helmholtz equation). This equation has the following form:

$$C(\mathbf{R}', n) = C^t(\mathbf{R}', n) - n^2 \int_v G(\mathbf{R}' - \mathbf{R}'', n) V(\mathbf{R}'') C(\mathbf{R}'', n) dv \quad (1)$$

where:  $C^t(\mathbf{R}', n)$  - spatial distribution of the  $n$ -th Fourier component of an incident wave, which is the solution of Helmholtz equation,  $C(\mathbf{R}', n)$  - the entire field (incident and scattered) in space,  $\mathbf{R}' \equiv [z, \mathbf{r}]'$  - vector of coordinates in space,  $\mathbf{R}'' \equiv [z, \mathbf{r}]''$  - vector of

coordinates in region  $\nu$  occupied by heterogeneities described by scattering potential  $V$ ,  $\mathbf{r} \equiv [x, y]$ .  $G(\mathbf{R}, n) = G(R, n) \equiv \exp(i \cdot n \cdot R) / 4\pi \cdot R$  is Green function of Helmholtz equation,  $R \equiv |\mathbf{R}|$ . Then independent variable normalization is applied so that speed of sound (average in the medium or of the medium surrounding  $V$ ) is  $\nu_0 = 1$ .

For the modeling purpose it is assumed that dispersion occurs on the point heterogeneity with elementary target strength which can take any coordinate  $\mathbf{R} \equiv [z, \mathbf{r}]$  in the imaging area. Then in (1) it is replaced  $V(\mathbf{R}'') = \nu \delta(\mathbf{R}'' - \mathbf{R})$ ,  $\nu = const$ , where  $\delta(\bullet)$  is the Dirac distribution,  $\nu$  is the 'target strength' of a point scatterer. The above assumption is sufficient for basic, correct analysis of transmit/receive characteristics of transducers and their combinations, which are important for this work, and is also used in literature.

Determined on the basis of solution (1) scattered field with target coordinate is given by

$$C^r(\mathbf{R}', \mathbf{R}, n) = -n^2 \nu G(\mathbf{R}' - \mathbf{R}, n) C^t(\mathbf{R}, n) . \quad (2)$$

The electric signal (here its Fourier spectrum) induced by the falling on the surface  $\Pi$  of the transducer scattered field and registered in the receive channel is described by the formula

$$\begin{aligned} E(\mathbf{R}, n) &= c^e(n) \cdot \int_{\Pi} C^r(\mathbf{R}', \mathbf{R}, n) d\Pi & E(\mathbf{R}, t) &= F^{-1}[E(\mathbf{R}, n)] \\ &= c^r \nu(n) n^2 g^r(\mathbf{R}, n) C^t(\mathbf{R}, n) = n^2 \nu c^r(n) g^r(\mathbf{R}, n) c^t(n) g^t(\mathbf{R}, n), \end{aligned} \quad (3)$$

where:  $c^r(n)$  is receiver frequency response, cumulating electromechanical and electric properties of the transducer and the registration channel;  $c^t(n)$  is the transmitted impulse spectrum. The transmit  $g^t$  and receive  $g^r$  characteristics are the solutions of Helmholtz equation according to Dirichlet and Neumann boundary value problems for  $z=0$  and in the half space  $z \geq 0$ . Their formulae are:

$$\begin{aligned} g^r(\mathbf{R}, n) &= \Pi(\mathbf{r}) \otimes_r G(\mathbf{R}, n) \\ g^t(\mathbf{R}, n) &= \Pi(\mathbf{r}) \otimes_r G^z(\mathbf{R}, n), \quad G^z(R, n) \equiv 2\partial_z G(R, n) \end{aligned} \quad (4)$$

where  $G^z$  is Green function for Dirichlet problem. It is assumed that the elementary transducer is evenly loaded and is of rectangular shape with dimensions  $a \times b$ . Then  $\Pi(\mathbf{r})$  are the characteristic functions of transducers simultaneously describing their loading (apodization).

$$\Pi(\mathbf{r}) \equiv \begin{cases} 1 & \text{for } -a/2 \leq x \leq a/2 \wedge -b/2 \leq y \leq b/2 \\ 0 & \text{for other } \mathbf{r} \end{cases} \quad (5)$$

The modelled  $L$  element linear array of identical elementary transmit-receive rectangular apertures located with pitch  $D$  on the plane  $z=0$  is shown in Fig.1.

In the methods of synthetic aperture construction the transmit function of a transducer is generally separated from its receive function. A part of the transducers from the array transmits and a part of them receives moreover these groups may have a common part – transducers which receive echoes of the signal transmitted by them. For two transducers, from

which  $l$ -th is in position  $\mathbf{r}_l = [0, x_l, 0]$  transmits and  $j$ -th in position  $\mathbf{r}_j = [0, x_j, 0]$  receives the dispersed in point  $\mathbf{R}$  signal, the spectrum of the registered in channel  $j$ -th echo has on the basis of (3) and (4) the following form

$$E(\mathbf{R}, n, l, j) \equiv v c^{rt}(n) g^r(\mathbf{R} - \mathbf{r}_j, n) g^t(\mathbf{R} - \mathbf{r}_l, n), \quad c^{rt} \equiv n^2 c^r c^t \quad (6)$$

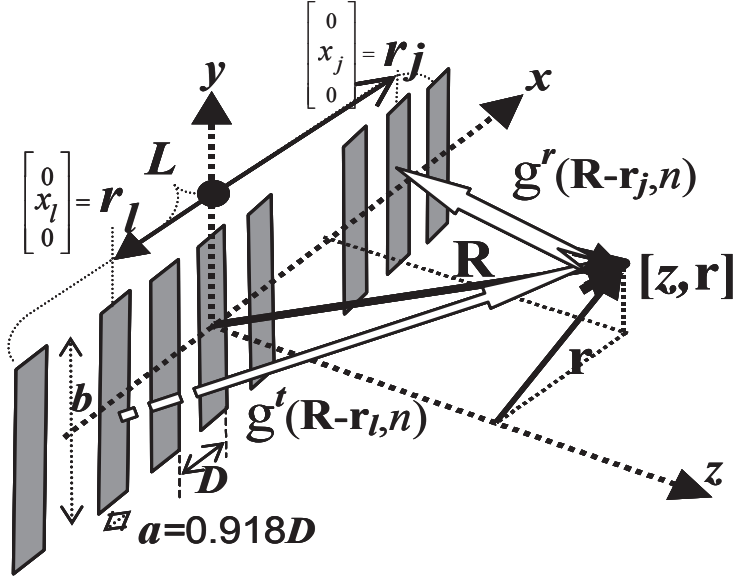


Fig.1. Initial linear array of transducers.  $D$ -pitch (distance between transducer centres).

Generally for the  $L$  element array there are  $M = M_{Tot} = (2^L - 1)^2$  different ways of transmitting and receiving dispersed signals (different bursts). It results from the number of  $L$  element pairs of sequences  $(\dots, \mathbf{0}, \dots, \mathbf{1}, \dots)$  determining elements active(1) in transmitting  $q_{t_l}^m$  and in receiving  $q_{r_j}^m$

$$\bigwedge_{m=1,2,\dots,M} (q_{t_l}^m, q_{r_j}^m) : l, j \rightarrow \{0;1\}; l, j = 1, 2, \dots, L \quad (7)$$

$m$  – numbers transmissions and receptions (bursts). The spectrum of the field dispersed in  $\mathbf{R}$  received by  $j$ -th transducer and registered in  $j$ -th channel after  $m$ -th burst is given by

$$E(\mathbf{R}, n, j; m) \equiv v c^{rt}(n) q_{r_j}^m g^r(\mathbf{R} - \mathbf{r}_j, n) \sum_l q_{t_l}^m g^t(\mathbf{R} - \mathbf{r}_l, n) \quad m = 1, 2, \dots, M (= M_{Tot}) \quad (8)$$

The structural matrix

$$Q_{j,l}^m \equiv q_{r_j}^m q_{t_l}^m \quad m = 1, 2, \dots, M \quad (9)$$

and the way of image reconstruction from  $M$  registered echoes (partial images) define the SA structure. As a result of echo registration (with spectra (8)) after each of  $m$ -th bursts the acquisition matrix with dimensions  $L \times \tau$  ( $\tau$  - number of time probes in each of  $L$  channels). It is assumed that in different comparable SAs the number  $\tau$  is identical, therefore it is omitted in valuation of memory necessary for acquisition. Each of the echoes described by (8)

provides information about the examined object but only few of them, obtained in a single ‘burst’, can be used to obtain an acceptable image of the object.

In practice, although it is possible to receive by all  $L$  transducers  $\bigwedge_{j=1,\dots,L} q_j^m = 1$ , because of technical reasons (and not only) in the formation of a transmitting beam in one burst not more than e.g.  $L/2$  transducers can be used and only properly grouped. For that and other reasons the result image is reconstructed from many elementary ones – corresponding to single ‘bursts’ of the acquisition matrix.

If we assume that (8) is a good model of an echo signal (spectrum) from the scatterer located in  $\mathbf{R} = \mathbf{R}_c$  and recorded in the  $j$ -th channel of the  $m$ -th acquisition matrix than the ideal image reconstruction  $P_i(\mathbf{R}, \mathbf{R}_c; m)$  assumes the existence of spectrum  $\bar{E}(\mathbf{R}, n, j; m)$  orthogonal to (8) relative to the position of scatterer  $\mathbf{R}_c$  and any point  $\mathbf{R}$  in space it means that

$$P_i(\mathbf{R}, \mathbf{R}_c; m) = \sum_j^L \sum_n \bar{E}(\mathbf{R}, n, j; m) E(\mathbf{R}_c, n, j; m) = \text{con}(L) \cdot \nu \delta(\mathbf{R} - \mathbf{R}_c) \quad (10)$$

Above it is assumed that there exists a possibility of compensation of all spectral factors in (8) in the whole range of the spectrum (if the band  $c^n(n)$  is limited the function similar to delta function is obtained). Because of the simplicity the standard reconstruction method is based on the approximation

$$\begin{aligned} \bar{E}(\mathbf{R}, n, j; m) &\cong \exp(-i \arg(g^r(\mathbf{R} - \mathbf{r}_j, n) \sum_l q_l^m g^t(\mathbf{R} - \mathbf{r}_l, n))) \\ &\approx \exp\left(-in\left(|\mathbf{R} - \mathbf{r}_j| + d(\mathbf{R}; m)\right)\right), \quad d(\mathbf{R}, m) \equiv \arg\left(\sum_l q_l^m g^t(\mathbf{R} - \mathbf{r}_l, n)\right) / n \end{aligned} \quad (11)$$

where  $d(\mathbf{R}; m)$  is effective (wave) range of the transmitting sequence  $q_l^m$  from point  $\mathbf{R}$  in the imaged area. According to our model the echo from the scatterer in  $\mathbf{R} = \mathbf{R}_c$  registered in  $j$ -th channel after  $m$ -th burst (in  $m$ -th acquisition matrix) has the following form

$$P(t, \mathbf{R}_c, j; m) \equiv P\left(t - (|\mathbf{R}_c - \mathbf{r}_j| + d(\mathbf{R}_c; m)), j; m\right) = F^{-1}\left[E(\mathbf{R}_c, n, j; m); t\right] \quad (12)$$

Placing (11) in (10) and adding up in groups of  $n$  means calculating inverse Fourier transform (12) for  $t = |\mathbf{R} - \mathbf{r}_j| + d(\mathbf{R}; m)$ . On the basis of (10) changing  $\mathbf{R}$  the combined image of the point scatterer located in  $\mathbf{R} \equiv \mathbf{R}_c$  is obtained.

$$P_i(\mathbf{R}, \mathbf{R}_c; m) = \sum_j^L P(\tau(\mathbf{R}, \mathbf{R}_c, j; m), j; m). \quad (13)$$

$$\tau(\mathbf{R}, \mathbf{R}_c, j; m) \equiv |\mathbf{R} - \mathbf{r}_j| + d(\mathbf{R}; m) - |\mathbf{R}_c - \mathbf{r}_j| - d(\mathbf{R}_c; m) \quad (14)$$

The image of the point scatterer is obtained as a result of adding up the fragments of the wave form recorded in the receive channels with the simultaneous compensation of their phases – distance from the transmitting sequence to the scatterer and to  $j$ -th detector. This is

the easier example of the dynamic focusing method. The meaningful image of the scatterer is obtained if the receiving sequence is long enough in the range of  $\mathbf{R}$  so that  $-0.5\tau p_j \leq \tau(\mathbf{R}, \mathbf{R}_c, j; m) \leq 0.5\tau p_j$  and the echo is strong enough,  $\tau p_j$  is the time echo lasts in the  $j$ -th channel. The discussion about the possibility of applying the general formula (11) on  $d()$  in the case of any  $q_{t_l}^m$  transmitting sequence is omitted. Because in practice the sequences which allow to apply approximations  $d()$  ‘in the real time’ and do not require considerable computational power are used.

Generally, the result image of the object is obtained by combining the images from all  $M$  bursts

$$\text{Pi}(\mathbf{R}, \mathbf{R}_c) = \sum_{m=1}^M \chi(\mathbf{R}; m) \text{Pi}(\mathbf{R}, \mathbf{R}_c; m) \quad (15)$$

In general coefficients of combination  $\chi$  may be complex functions. Most often these are the masking functions formally defining a part of the entire imaged field, which appears as a result of the  $m$ -th burst (from the  $m$ -th acquisition matrix). In the STA presented below [3]

$$\chi(\mathbf{R}, m) \equiv \text{rect}(x - xt_m / \Delta x; 0 < z \leq z_{\max}, y = 0) \quad (16)$$

i.e. for every  $m$  there is a unit step function in the rectangle  $\{xt_m - \Delta x < x \leq xt_m + \Delta x; 0 < z \leq z_{\max}; y = 0\}$ . Additionally, it is assumed that  $|xt_m - xt_{m-1}| = 2\Delta x$  which means that the entire image is the complementary sum of (not overlapping)  $M$  partial images created by the  $m$ -th acquisition matrix.

In the presented CSTA all  $\chi(\mathbf{R}, m) \equiv 1$  for every  $\mathbf{R}$ . In this case adding images can be substituted by adding echoes (12). After each  $m$ -th burst the echoes are added in each of  $j$  channels to the echoes existing after the  $m-1$ -th burst. This way instead of  $M$  acquisition matrices we have only one which is used to create an image. The  $M$ -layer three-dimensional structural synthetic aperture matrix (9) corresponds to one-layer two-dimensional

$$Q_{j,l} \equiv \sum_{m=1}^M q r_j^m q t_l^m, \quad (17)$$

describing the effect equivalent to  $M$  bursts. In the case of CSTA the formula of image creation has the following form

$$\text{Pi}(\mathbf{R}, \mathbf{R}_c) = \sum_j^L P(\tau(\mathbf{R}, \mathbf{R}_c, j), j), \quad (18)$$

$$P(\tau(\mathbf{R}, \mathbf{R}_c, j), j) \equiv \sum_m^M P\left(t - |\mathbf{R}_c - \mathbf{r}_j| + d(\mathbf{R}_c, m), j; m\right) \Big|_{t=|\mathbf{R}-\mathbf{r}_j|+dc(\mathbf{R})}. \quad (19)$$

where  $P(\tau, j)$  corresponds to one acquisition matrix. In CSTA  $dc(\mathbf{R})$  function is of the same significance as  $d(\mathbf{R}, m)$  in STA but it is not dependent on  $m$ . It has to be noticed that the number of  $M$  in the case of CSTA can be considerably smaller than in the first case i.e. standard STA. The results obtained using both imaging methods are presented below.

## 2. DESCRIPTION OF THE METHODS

In the conducted numerical and experimental study (in the range of presented here results) for both methods the identical for every  $m$  (burst) receiving sequences with the maximum number of active in reception transducers  $Lr=L$  ( $=64$ )  $\wedge_{j=1,\dots,L} q_{r_j}^m = 1$  were used. The of transmitting sequences are defined as follows

$$q_{t_l}^m \equiv \begin{cases} 1 & \text{for } 1 \leq l_m + 1 \leq l \leq l_m + Lt \leq L \\ 0 & \text{for other } l \end{cases} \quad \begin{aligned} l_m &\equiv (m-1) \cdot sh \\ m &= 1, 2, \dots, M \equiv \frac{L-Lt}{sh} + 1 \end{aligned} \quad (20)$$

and are compact and identical for both methods sequences of active in transmission transducers.

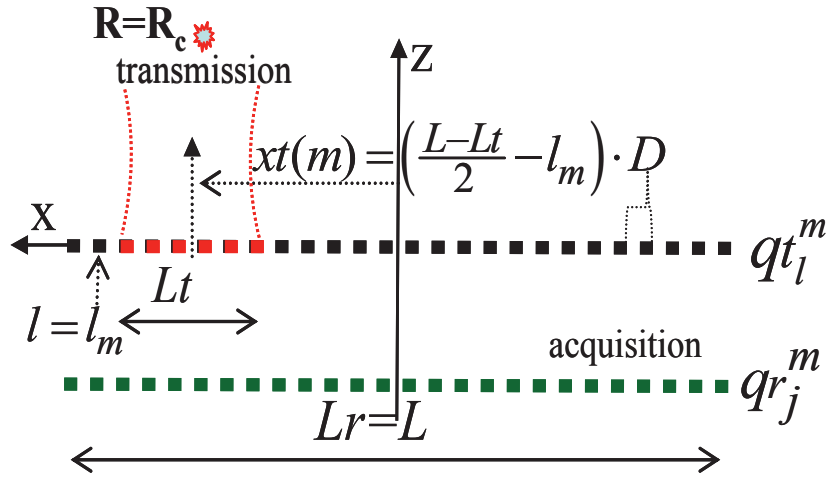


Fig.2. Diagram of transmitting and receiving sequence for certain  $m$ .

For CSTA it is assumed that  $sh = Lt (=16)$  which on the basis of (20) gives  $M = L/Lt (=4)$ . Other CSTAs for which  $sh < Lt$  are also possible. This type of CSTA minimizes the number of bursts for certain  $Lt$ . For the traditional STA  $sh=2$ ,  $Lt=16$  and respectively  $M=25$ .

As a result of spectral analysis of formulae from section 1 (omitted here because of its extensiveness) the form  $dc(\mathbf{R}_c; m) dc(\mathbf{R}; m)$  was determined which compensates the distance from  $m$ -th transmitting sequence to the scatterer in  $\mathbf{R}=\mathbf{R}_c$ . Its form is not dependent on  $m$  according to the idea of creating image from one acquisition matrix Eqs. 18, 19. It depends (to some extent) on the size of the b-elevation of transducer. To give an approximate value  $dc(\mathbf{R}, m) = dc(\mathbf{R}) \cong z$ .

For the traditional STA  $d(\mathbf{R}; m) \cong \sqrt{(x - xt(m))^2 + z^2}$  is applied,  $xt_m = xt(m)$  is the position of the centre line of the  $m$ -th partial image and also the centre of the  $m$ -th transmitting sequence. It has to be noticed that for narrow partial images or for the images, where  $|x - xt_m| \leq \Delta x \ll z$ ,  $d(\mathbf{R}; m) \cong z$  is also obtained. In this work it is assumed that  $\Delta x \equiv D (=0.3048 \text{ mm})$ .



The diagrams in Fig.3. illustrate the subsequent m-sequences of the transmission, respective acquisition sequences and acquisition matrices and the characteristic way of image creation.

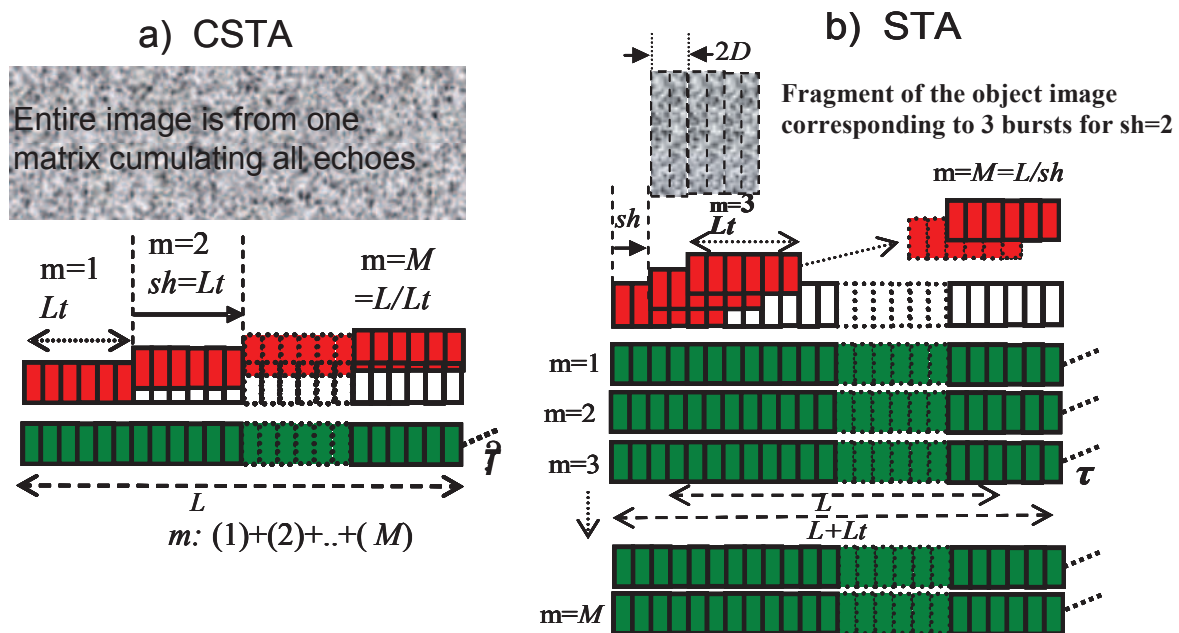


Fig.3. Diagrams of transmission, acquisition and imaging in : a) CSTA – on the left and b) STA – on the right. Transmitting sequences are red, receiving transducers and acquisition matrices – green.

The characteristic feature of CSTA is that independent on the way of transmitting (the number of transmissions  $M$ ) all echoes are collected in one  $L \times \tau$  matrix ( $L$ - number of channels - receiving transducers;  $\tau$  - the number of echo samples in each of  $1 \leq l \leq L$  channels). From the echo samples collected in this matrix according to formula (18) the entire image of the object at least  $L$  lines in width is created. Moreover, the information about the position of transmitting sequence ( $xt(m)$ ) is not needed to calculate time delays from the transmitting sequence to the scatterers. In the simplest version the sequence of  $Lt$  transducers transmits simultaneously. It is assumed that such natural number  $M$  - number of transmissions - bursts is chosen that  $L = M \cdot Lt$ . After each of  $m = 1, 2, \dots, M$  bursts the echo samples are recorded in the described above matrix and added to the existing after the previous  $m-1$ -th burst and the transmitting sequence is shifted by  $sh=Lt$  transducers Fig.3.a). This is a particular case of STA. In other SA cases the echo acquisition in separate for every burst matrices is applied. Namely if we want to create the  $L$ -line wide image ( $L \cdot D$  mm) transmitting by  $Lt$  transducers (transmitting sequences have to be  $L+Lt$  long) than after each  $m$ -th burst the  $m$ -th acquisition matrix is created and the transmitting sequence is shifted by  $sh$  lines ( $sh \cdot D$  mm) (scanning with  $sh$  shift). The entire image is created from  $M=(L/sh)$  partial images according to formula (15), each  $sh$  lines in width ( $sh \cdot D$  mm) corresponding to centre lines of transmitting sequences. The memory and time needed for image reconstruction are characterized by numbers  $\sim(L+Lt)(L/sh)$  Time  $\sim M=(L/sh)$  Fig.1.b). In the discussed CSTA case Mem  $\sim L$  Time  $\sim M=L/Lt$ , respectively.



### 3. EXPERIMENTAL RESULTS

The comparative experiments were carried out on the wire phantom immersed in water and RMI tissue mimicking phantom in conditions similar to real study. The programmable ultrasound scanner ULTRASONIX enabling creation of different multielement SAs in the band of 5 MHz was used for synthesis of transmitted impulses and for acquisition of RF signals. The images were created from RF data on standard PCs according to formulae (18) for CSTA and (15) for STA. The experimental setup is shown in Fig.4.

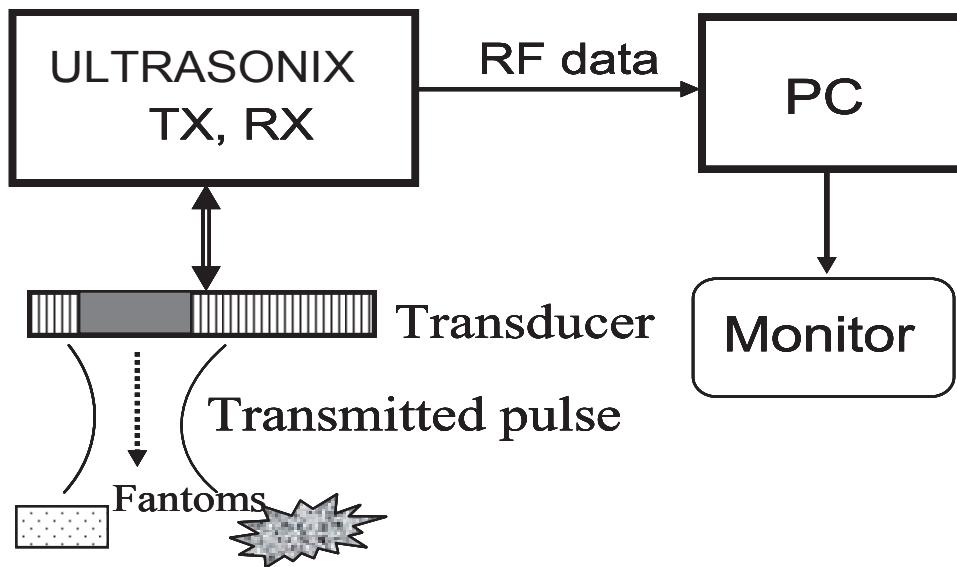


Fig.4. Experimental setup.

The results of comparative experiments are presented below – images of wire and tissue mimicking phantoms obtained by the described CSTA and STA methods. No special methods of improving image quality were used. The signal controlling the brightness of imaged pixels is  $|\text{Pi}(\mathbf{R}, \mathbf{R}_c)|$  for formulae (18)- CSTA and (15)- STA.

Normalizing to 1 imaged signals was applied.

It should be noted that because the image width in the described STA ( $L(64)$  element head) is equal to  $M \cdot sh = 50$  Lines ( $= 50 \cdot 0.3 \text{mm} = 15 \text{mm}$ ) the image is narrower than the basic width of the image in CSTA  $L=64$  lines ( $= 19.2 \text{mm}$ ). In the experiment the imaging field was widened to 80 lines ( $= 80D = 24 \text{mm}$ ) for CSTA.

**A) Wire phantom in water**

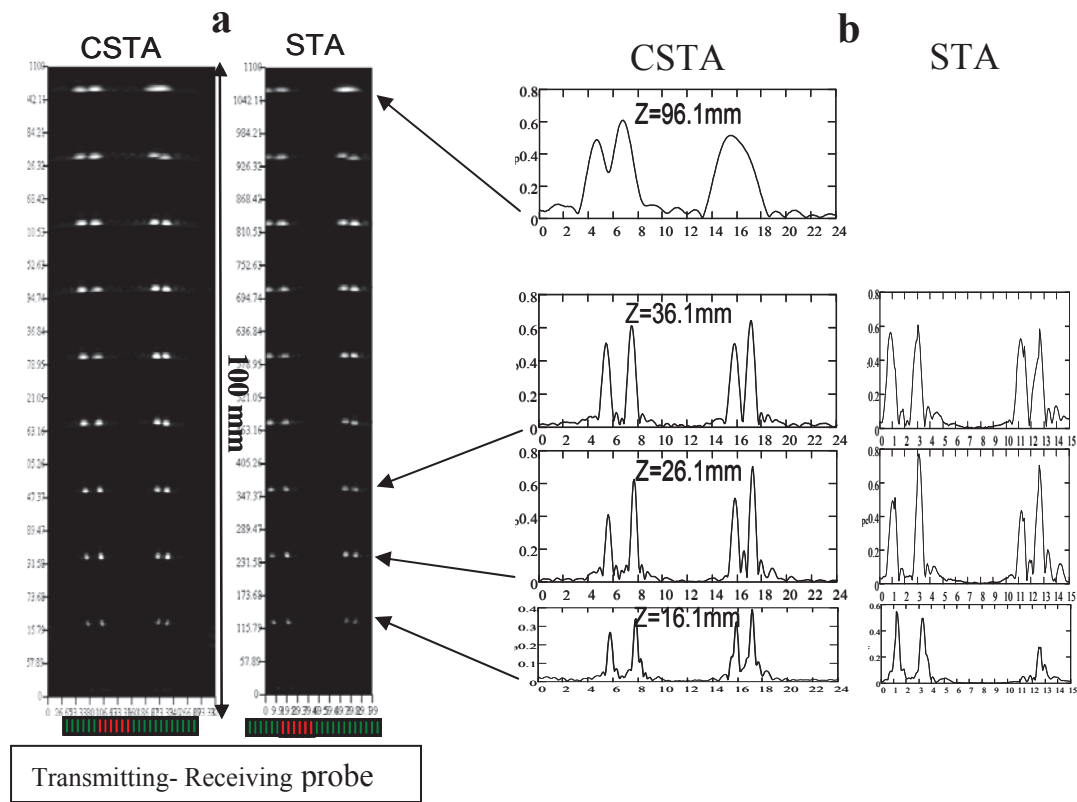


Fig.5. a) Images of wire phantom immersed in water. Linear grey scale. b) Cross-section at marked by arrows depths  $z$ .

**B) Tissue mimicking phantom with wires (RMI)**

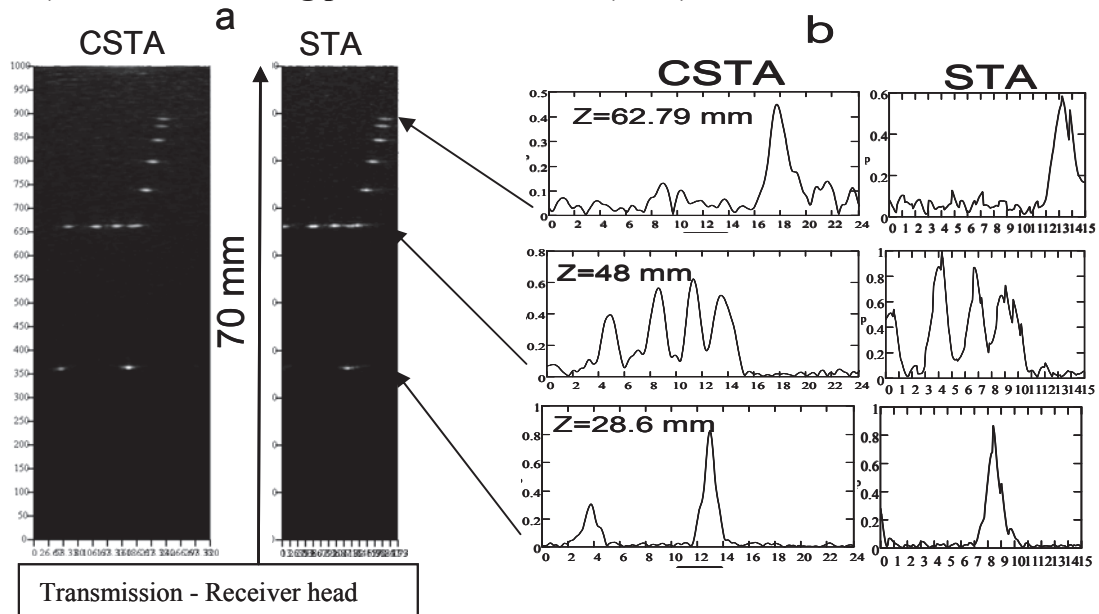


Fig.6.a) Images of tissue mimicking phantom in water in linear grey scale. b) Cross-section at depths  $z$ .

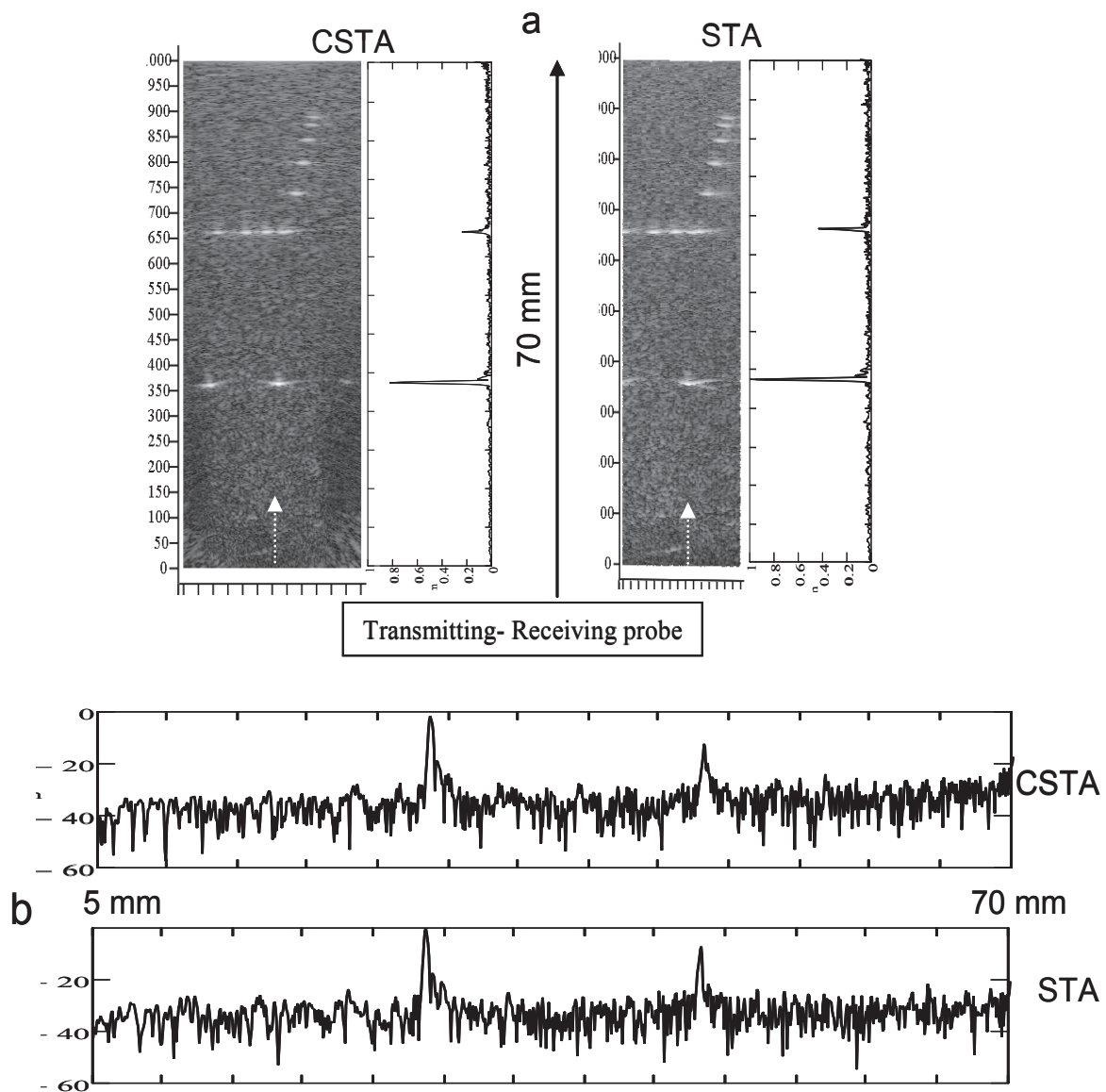


Fig.7. a) Images of tissue mimicking phantom with wires in logarithmic grey scale. Specles determine signal level of tissue background. On the right of images – in linear scale charts of signal level along white arrows  $x=0.9\text{mm}$ . b) Charts of signal level along marked directions in logarithmic scale.

#### 4. CONCLUSION

The presented results allow to conclude that CSTA is “locally” optimal method (in the sense mentioned in the introduction). It allows to expect that this method can be used in cheap not having considerable computing power imaging platforms. Moreover it can be expended to  $Lr=2,3 \times L$  (CSTRA) R- Receive.

#### ANKNOLEDGMENTS

This work has been supported by the Ministry of Science and Higher Education, Poland (Grant No. N N518 503339).

## REFERENCES

- [1] T. Kujawska, J. Wojcik, A. Nowicki, Temperature fields induced in rat liver in vitro by pulsed low intensity focused ultrasound, *Hydroacoustics* vol. 13, pp. 153-162, 2010.
- [2] I. Trots, A. Nowicki, M. Lewandowski, Synthetic transmit aperture in ultrasound imaging, *Archives of Acoustics*, vol. 43, no. 4, pp. 685–695, 2009.
- [3] A. Nowicki, *Ultradźwięki w medycynie*, 226, Warszawa 2010.